Logarithmic terms in atom-surface potentials: Limited applicability of rational approximations for intermediate distance

U. D. Jentschura and C. Moore
Department of Physics and LAMOR, Missouri University of Science and Technology, Rolla, Missouri 65409, USA

(Received 17 May 2023; accepted 21 June 2023; published 19 July 2023)

It is usually assumed that interaction potentials, in general, and atom-surface potential, in particular, can be expressed in terms of an expansion involving integer powers of the distance between the two interacting objects. Here, we show that, in the short-range expansion of the interaction potential of a neutral atom and a dielectric surface, logarithms of the atom-wall distance appear. These logarithms are accompanied with logarithmic sums over virtual excitations of the atom interacting with the surface in analogy to Bethe logarithms in quantum electrodynamics. We verify the presence of the logarithmic terms in the short-range expansion using a model problem with realistic parameters. By contrast, in the long-range expansion of the atom-surface potential, no logarithmic terms appear, and the interaction potential can be described by an expansion in inverse integer powers of the atom-wall distance. Several subleading terms in the large-distance expansion are obtained as a byproduct of our investigations. Our findings explain why the use of simple interpolating rational functions for the description of the atom-wall interaction in the intermediate regions leads to significant deviations from exact formulas.

DOI: 10.1103/PhysRevA.108.012815

I. INTRODUCTION

A. Motivation

We investigate the Casimir-Polder (CP) interaction potential [1] between an atom and a dielectric surface, which arises due to quantum fluctuations of the electromagnetic field. As well known, (see Refs. [2–4]), the dominant term of the interaction mediated by the dipole polarizability in the short-range limit is of the form

$$V(z) \approx -\frac{C_3}{z^3}, \quad z \ll \frac{a_0}{\alpha}, \tag{1}$$

where z is the atom-wall distance, α is the fine-structure constant, a_0 is the Bohr radius, and C_3 is a constant coefficient. In the long-range limit, retardation effects become important, and the dipole contribution to the atom-wall potential is described by the formula,

$$V(z) \approx -\frac{C_4}{z^4}, \quad z \gg \frac{a_0}{\alpha}, \tag{2}$$

where C_4 also is a constant coefficient. Atom-surface interactions are particularly interesting with regard to quantum reflection [5,6]. The functional form of atom-surface interactions has been verified for cavities [7,8], confirming theoretical predictions [9,10]. It has been an interesting problem studied in Ref. [11] to find a suitable functional form for the interpolation between the $1/z^3$ and the $1/z^4$ regimes. The corresponding (dimensionless) interpolating function after dividing out the leading short-range term has been termed the *shape function* [see Eqs. (34) and (35) of Ref. [11]]. One particularly simple functional form, which encompasses the interpolation, has been discussed in the literature (see Refs. [5,11,12]),

$$V(z) \approx \frac{C_4}{z^3(z+\ell)}, \quad C_3 \approx \frac{C_4}{\ell}, \tag{3}$$

where the second approximate relation is a consequence of the first. Here, ℓ is a parameter, of order $a_0/\alpha \approx 137\,a_0$, which describes the transition point between the short-range and the long-range asymptotics. The functional form (3) constitutes a very simple rational interpolation between the short-range and the long-range asymptotics, regimes of the CP interaction.

For (perfectly) conducting surfaces, in the transition region $z \approx a_0/\alpha$, a numerical evaluation of the complete expression for the atom-wall interaction potential, in general, shows good agreement with the interpolating form given in Eq. (3) as described in Refs. [3,5,11,13]. However, for realistic materials, the simple interpolating model (3) is less suitable to describe the transition region $z \approx a_0/\alpha$. Substantial deviations are observed in the transition region $z \approx a_0/\alpha$. Here, we argue that the difficulties in adequately approximating the exact potential with a rational function are not accidental, and find a natural explanation in the presence of logarithmic terms in the short-range limit, which defy an accurate representation or even approximation by a simple rational function. In particular, we find that the simple interpolating form given in Eq. (3) is not able to represent the exact atom-wall potential in the regime of intermediate atom-wall distances because of the presence of logarithmic terms in the short-range expansion, which are hard to approximate by a rational function of the atom-wall distance (see also Fig. 6).

This paper is organized as follows. The (semi-)analytic structure of the short-range expansion of the atom-surface potential (which involves logarithms of the atom-wall distance) is analyzed in Sec. II. Numerical evaluations of the potential

and the verification of the analytic short-range coefficients are discussed in Sec. III. The long-range coefficients of the atom-surface potential are analyzed in Sec. IV, and numerical calculations are presented in Sec. V. Conclusions are reserved for Sec. VI. Système International (SI) mksA units will be adopted in the following except for the numerical calculations reported in Secs. III and V where we switch to the atomic unit system.

B. Expansions involving logarithms

We here argue that the correct short-range expansion of the atom-wall interaction can be written in the following form:

$$V(z) = -\sum_{(3\geqslant n\geqslant 0)j} \frac{C_{nj}}{z^n}\left[\ln\left(\frac{2\alpha z}{a_0}\right)\right]^j - \sum_{(n>0)j} \overline{C}_{nj}\, z^n \left[\ln\left(\frac{2\alpha z}{a_0}\right)\right]^j, \tag{4}$$

which is a semianalytic expansion in powers of the atom-wall distance z and in powers of the logarithm $\ln(2\alpha z/a_0)$. The expansion (4) is valid for $z \ll \frac{a_0}{\alpha}$. The first index n of the short-range C_{nj} coefficients corresponds to the inverse power of the atom-wall distance z (functional form z^{-n}), whereas, the second index j gives the power of the logarithm $\ln(2\alpha z/a_0)$. The dominant term is obtained for $n = 3$ and $j = 0$ and reads as $-C_{30}/z^3$. It is of note that the presence of a logarithm numerically enhances a term in the limit $z \to 0$, i.e., a contribution proportional to C_{11} parametrically dominates a contribution proportional to C_{10}. The C_3 coefficient from Eq. (1) qualifies itself as the C_{30} coefficient in the semianalytic expansion given in Eq. (4). Subleading terms involve powers z^{-n} with $0 \leqslant n < 3$. Furthermore, the coefficients $\overline{C}_{nj}$ multiply terms involving positive powers of z, and are, thus, proportional to z^n. They also involve the jth power of the logarithm $\ln(2\alpha z/a_0)$. In other words, when the power of the atom-wall distance z is positive, we add a bar over the C coefficient.

The expansion (4) can be written in terms of a sum of terms $\mathcal{P}_{nj}(z)$ (describing terms proportional to z^{-n} with integer n) and $\overline{\mathcal{P}}_{nj}(z)$ (describing terms proportional to z^n with integer n),

$$V(z) = \sum_{(n\geqslant 0)j} P_{nj}(z) + \sum_{(n\leqslant 0)j} \overline{P}_{nj}(z), \tag{5a}$$

$$P_{nj}(z) = -\frac{C_{nj}}{z^n}\left[\ln\left(\frac{2\alpha z}{a_0}\right)\right]^j, \tag{5b}$$

$$\overline{P}_{nj}(z) = -\overline{C}_{nj}\, z^n \left[\ln\left(\frac{2\alpha z}{a_0}\right)\right]^j. \tag{5c}$$

Specifically, for a nonperfect conductor in the limit $z \to 0$, the short-range expansion has the functional form

$$V(z) = -\frac{C_{30}}{z^3} - \frac{C_{11}}{z}\ln\left(\frac{2\alpha z}{a_0}\right) - \frac{C_{10}}{z} - C_{01}\ln\left(\frac{2\alpha z}{a_0}\right) - C_{00} - \overline{C}_{12}\, z\, \ln^2\left(\frac{2\alpha z}{a_0}\right) + O[z\ln(z)]. \tag{6}$$

We here list the terms in ascending parametric order in the regime $z \ll a_0/\alpha$. The results for the leading and subleading terms (proportional to C_{30} and C_{11}) can be found in Eqs. (35) and (37), respectively. We here suppress, in the notation, a possible temperature dependence of the coefficients, which could be caused by the explicit temperature dependence of the optical response of the medium (see, e.g., Ref. [14]). It is somewhat surprising that for a realistic dielectric function, which describes a (necessarily) nonperfect conductor, the term of order $1/z^2$ vanishes. By contrast, in the limit $\epsilon(\omega) \to \infty$ one obtains a nonvanishing $1/z^2$ term (see Appendix A). Expressed differently, the limit $\epsilon(\omega) \to \infty$ is approached nonuniformly (see also Ref. [4]). Some of the nonlogarithmic coefficients in the short-range expansion (6), notably the coefficients C_{10} and C_{00}, involve logarithmic sums over virtual excitations of the atom, much in analogy to the well-known Bethe logarithm correction in atomic systems [15,16].

In the long-range limit, the appropriate expansion involves inverse powers of the atom-wall distance (no logarithmic terms) of the functional form z^{-n}. The terms up to subsubleading order are

$$V(z) = -\frac{C_4}{z^4} - \frac{C_5}{z^5} - \frac{C_6}{z^6} + O\left(\frac{1}{z^7}\right). \tag{7}$$

The expansion (7) is valid in the regime $z \gg \frac{a_0}{\alpha}$. The long-range expansion is an expansion in inverse powers of n. Both Secs. III and V include numerical examples, which verify the accuracy of the (semi-)analytic expansions given in Eqs. (7) and (6).

II. SHORT-RANGE ASYMPTOTICS

A. General considerations

For a material with an angular-frequency-dependent dielectric function $\epsilon(\omega)$, the atom-wall interaction potential $V(z)$ the can be written as follows (see Refs. [3,13] and Chap. 5 of Ref. [17]):

$$V(z) = \mathcal{Q}\int_0^\infty d\omega\, \alpha(i\omega)\omega^3 \int_1^\infty dp\, H[\epsilon(i\omega), p]\, e^{-2\omega p z/c},$$
$$\mathcal{Q} = -\frac{\hbar}{8\pi^2\epsilon_0 c^3}, \tag{8}$$

where $H = H[\epsilon(i\omega), p]$ is defined in Eq. (9). The dipole polarizability $\alpha(\omega)$ of the atom is evaluated at imaginary angular frequency argument. The atomic reference state is assumed to be the ground state; for an excited reference state, the derivation becomes more complex (see Ref. [18]). For completeness, we note that $\hbar$ is the reduced Planck constant, the vacuum permittivity is ϵ_0, and the speed of light is c. The H function is given as follows,

$$H(\epsilon, p) = \frac{\sqrt{\epsilon - 1 + p^2} - p}{\sqrt{\epsilon - 1 + p^2} + p} + (1 - 2p^2)\frac{\sqrt{\epsilon - 1 + p^2} - p\epsilon}{\sqrt{\epsilon - 1 + p^2} + p\epsilon}. \tag{9}$$

A remark is in order. In principle, $\epsilon(\omega)$ could depend on other variables, such as the temperature of the material. external pressure applied to the crystal, or, the concentration of impurities or dislocations in the crystal structure. If P is the pressure and η is the concentration of impurities, then our notation

$\epsilon = \epsilon(i\omega)$ is taken to describe a functional relation of the form

$$\epsilon(i\omega) \equiv \epsilon(T_\Delta, P, \eta, \ldots; i\omega). \tag{10}$$

The dimensionless parameter $T_\Delta = (T - T_0)/T_0$ has been used in Ref. [14] in order to investigate the temperature dependence of the dielectric function (T_0 denotes a reference temperature, taken as the room temperature in Ref. [14]).

A further practical remark on the two-dimensional numerical integration of Eq. (8) also is in order. Namely, the numerical integration of Eq. (8) can prove to be a little more difficult than one would initially assume. For the convenience of the reader, we may point out that numerically accurate results were obtained when we used Gaussian numerical quadrature methods adapted to the problem at hand. Specifically, we used Gauss-Legendre quadrature [19] for the regime of low p variable in Eq. (8), and Gauss-Laguerre quadrature [19] for the exponential tail in the p variable in Eq. (8), followed by a substitution in the ω variable, which maps the interval $\omega \in (0, \infty)$ to the interval $t \in (0, 1)$ where, for example, $\omega = \omega_0 t/(1-t)$, and ω_0 is a suitably chosen parameter of order unity in atomic units. The t variable could then be integrated over using Gauss-Legendre quadrature.

We are interested in the short-range asymptotics of the interaction potential $V(z)$ for the range of $z \ll a_0/\alpha = \hbar/(\alpha^2 mc)$, where m is the electron mass. In this range, the exponential damping due to $\exp(-2\omega pz/c)$ is not very pronounced. Typical atomic angular frequencies are in the range of $\omega \sim \alpha^2 mc^2/\hbar$. In this range of frequencies, one has $\omega z/c \ll 1$ for $z \ll a_0/\alpha$. Contributions from large ω are, thus, not significantly suppressed, and the region of large p and ω contributes significantly to the integral.

The expansion for $z \ll a_0/\alpha$ has to be approached with extreme care. We first consider the integral over p where the integration region is the interval $p \in (1, \infty)$. The presence of the exponential factor $\exp(-2\omega pz/c)$ and the fact that we are integrating from $p = 1$ to $p = \infty$ (as opposed to starting the integration at $p = 0$) ensures that the exponential damping is still prevalent for small z, even if the exponential damping is not very pronounced. We will need the exponential suppression due to the factor $\exp(-2\omega z/c)$, which is still present after p integration, in order to ensure the convergence of the ω integral. Thus, we cannot simply expand the exponential $\exp(-2\omega pz/c)$ in powers of its argument.

However, we can expand the function $H(\epsilon(i\omega), p)$ for large p, and integrate over p, while keeping the exponential factor $\exp(-2\omega pz/c)$. We then apply the method of the overlapping parameter (see Chap. 4 of Ref. [17]) to the resulting integral over ω. (The only caveat connected with the expansion of the function $H(\epsilon(i\omega), p)$ for large p is that it is invalid in the integration interval around $p \sim 1$. This fact will give rise to an extra term to be discussed in Sec. II D; but let us not worry about this aspect at the current stage of the derivation.) For the ω integration, we introduce a scale-separation parameter $\omega = \Lambda/\hbar$, where Λ has dimension of energy. We then consider the low-energy part (LEP) and the high-energy part (HEP) of the virtual photon energy integrals,

$$\text{LEP: } \omega \in (0, \Lambda/\hbar), \quad \text{HEP: } \omega \in (\Lambda/\hbar, \infty), \tag{11}$$

where Λ acts as an ultraviolet regulator for the low-energy part and as an infrared regulator for the high-energy part. In the low-energy part, one can expand the exponential,

$$\exp\left(-\frac{2\omega z}{c}\right) = 1 - \frac{2\omega z}{c} + O\left(\frac{\omega z}{c}\right)^2, \tag{12}$$

in powers of its argument. The atom-wall distance is on the order of $z \sim a_0 \ll a_0/\alpha$ for the short-range expansion. At the overlapping (transition) parameter $\omega \sim \Lambda/\hbar$, the expansion breaks down, and we have

$$\frac{\Lambda z}{\hbar c} \sim \frac{\Lambda a_0}{\hbar c} \sim 1, \quad \Lambda \sim \frac{\hbar c}{a_0} = \alpha mc^2 = \frac{1}{\alpha} E_h, \tag{13}$$

where $E_h = \alpha^2 mc^2$ is the Hartree energy, which is unity when measured in atomic units.

The atomic polarizability varies appreciably over the angular frequency range $0 < \omega < E_h/\hbar$. In the high-energy part, where $\omega \in (\Lambda/\hbar, \infty)$, we can, thus, expand the atomic polarizability for large argument ω.

Finally, we expand both the high- as well as the low-energy parts, first in z for small z, then in Λ for large Λ, keeping only terms that are divergent in the limit of large Λ. The dependence on Λ cancels out because Λ only constitutes an artificial scale-separation parameter (for an illustration of the method, see Chap. 4 of Ref. [17] and Appendix B).

In order to consider the high-energy contributions to the short-range expansion of the atom-surface potential, the dielectric function and the dynamic polarizability are expanded in the following form:

$$\alpha(i\omega) = \frac{\alpha_2}{\omega^2} + \frac{\alpha_4}{\omega^4} + O(\omega^{-4}). \tag{14}$$

This equation implicitly defines the coefficients α_2 and α_4. For the dielectric function, we write the following asymptotic expansion for large ω:

$$\epsilon(i\omega) = 1 + \frac{\Omega_1}{\omega} + \left(\frac{\Omega_2}{\omega}\right)^2 + \left(\frac{\Omega_3}{\omega}\right)^3 + O\left(\frac{1}{\omega^4}\right). \tag{15}$$

Some remarks are in order. The coefficients $\Omega_{1\text{–}3}$ are defined so that they have the same physical dimension, namely, that of an angular frequency. The coefficient Ω_3 is defined to be real rather than complex, which means that if the coefficient of order ω^{-3} in the expansion of $\epsilon(i\omega)$ is negative, then Ω_3 is negative too. One might ask if the coefficient Ω_1 could be nonvanishing for typical functional forms of the dielectric function. For example, if one assumes, at least, in the regime of large ω, a Sellmeier functional form [20]

$$\epsilon(\omega) \approx \sum_k \frac{a_k\, \omega_k^2}{\omega_k^2 - \omega^2 - i\omega\gamma_k}, \tag{16}$$

with fixed parameters a_k, ω_k, and γ_k, then $\Omega_1 = 0$, and

$$(\Omega_2)^2 = \sum_k a_k\, \omega_k^2. \tag{17}$$

However, when we use a Lorentz-Dirac form [14,21–23]

$$\epsilon(\omega) = \sum_k \frac{a_k\left(\omega_k^2 - i\gamma_k'\omega\right)}{\omega_k^2 - \omega^2 - i\omega\gamma_k}, \tag{18}$$

then the oscillator strength in the numerator becomes a complex frequency-dependent quantity. In this case, the parameter

Ω_1 is nonvanishing,

$$\Omega_1 = \sum_k a_k \gamma'_k, \quad (\Omega_2)^2 = \sum_k a_k \bigl(\omega_k^2 - \gamma_k \gamma'_k\bigr), \tag{19}$$

where if the width of the resonances is small, one can assume that $\gamma_k\, \gamma'_k \ll \omega_k^2$.

B. Derivation of the leading coefficients

We concentrate on the derivation of the short-range expansion of the atom-surface potential with a particular emphasis on the three leading terms from Eq. (6) in the short-range limit,

$$V_{\rm SR}(z) \approx -\frac{C_{30}}{z^3} - \frac{C_{11}}{z} \ln\left(\frac{2\alpha z}{a_0}\right) - \frac{C_{10}}{z} + O[z\,\ln(z)]. \tag{20}$$

Our goal is to discuss, in some detail, the derivation of the coefficients C_{30}, C_{11}, and C_{10}, which constitute the leading coefficients in Eq. (6). These terms will need to be extracted from Eqs. (8) and (9). This constitutes a nontrivial exercise. The short-range asymptotics of the atom-wall potential are obtained from the contribution of high-energy virtual photons (high ω) and large integration variables p. The exponential suppression factor $\exp(-2\omega p z/c)$ cuts off the ultraviolet divergences of the integrals over ω and p, and it is, thus, necessary to keep this term in unexpanded form; a Taylor expansion of the exponential $\exp(-2\omega p z/c)$ in powers of z leads to problems in the ultraviolet integration region of large ω. Hence, one proceeds as follows.

First, one expands the function $H(\epsilon(i\omega), p)$ for large p, leading to

$$H(\epsilon, p) = S(\epsilon, p) + O(p^{-6}), \tag{21}$$

where

$$\begin{aligned} S(\epsilon, p) = 2p^2 \frac{\epsilon - 1}{\epsilon + 1} &- \frac{(\epsilon - 1)\,(3\epsilon + 1)}{(\epsilon + 1)^2} \\ &+ \frac{(\epsilon - 1)\,(3\epsilon^3 + 11\epsilon^2 + \epsilon + 1)}{4p^2(\epsilon + 1)^3} \\ &+ \frac{(\epsilon - 1)^2\,(3\epsilon^4 + 12\epsilon^3 + 16\epsilon^2 + 1)}{8p^4(\epsilon + 1)^4}. \end{aligned} \tag{22}$$

For the calculation of the leading analytic terms, one uses the result,

$$\int_1^\infty dp\, e^{-\frac{2\omega z p}{c}} S(\epsilon, p) = f_1(\epsilon, \omega) + f_2(\epsilon, \omega) + f_3(\epsilon, \omega). \tag{23}$$

The functions $f_i(\epsilon, \omega)$ with $i = 1$–3 are given as follows:

$$\begin{aligned} f_1(\epsilon, \omega) = e^{-2\omega z/c} \Biggl\{ &\left[\frac{1}{2}\left(\frac{c}{\omega z}\right)^3 + \left(\frac{c}{\omega z}\right)^2\right] \frac{\epsilon - 1}{\epsilon + 1} \\ &- \frac{c}{\omega z}\left(\frac{\epsilon - 1}{\epsilon + 1}\right)^2 + g(\epsilon) + \left[\frac{\omega z}{c} - \left(\frac{\omega z}{c}\right)^2\right] h(\epsilon) \Biggr\}, \end{aligned} \tag{24}$$

$$f_2(\epsilon, \omega) = \frac{\omega z}{c} \frac{(\epsilon - 1)\,(3\epsilon^3 + 11\epsilon^2 + \epsilon + 1)}{2(\epsilon + 1)^3} \,{\rm Ei}\left(-\frac{2\omega z}{c}\right), \tag{25}$$

$$f_3(\epsilon, \omega) = -\left(\frac{\omega z}{c}\right)^3 h(\epsilon)\,{\rm Ei}\left(-\frac{2\omega z}{c}\right), \tag{26}$$

$$g(\epsilon) = -\frac{(\epsilon - 1)(3\epsilon^5 - 9\epsilon^4 - 80\epsilon^3 - 88\epsilon^2 - 11\epsilon - 7)}{24(\epsilon + 1)^4}, \tag{27}$$

$$h(\epsilon) = \frac{(\epsilon - 1)^2\,(3\epsilon^4 + 12\epsilon^3 + 16\epsilon^2 + 1)}{24(\epsilon + 1)^4}. \tag{28}$$

One defines the potential,

$$\begin{aligned} V_S(z) &= Q \int_0^\infty d\omega\, \omega^3 \alpha(i\omega) \int_1^\infty dp\, S[\epsilon(i\omega), p] e^{-2\omega z p/c} \\ &= V_1(z) + V_2(z) + V_3(z), \end{aligned} \tag{29}$$

where

$$V_1(z) = Q \int_0^\infty d\omega\, \omega^3 \alpha(i\omega) f_1[\epsilon(i\omega), p], \tag{30a}$$

$$V_2(z) = Q \int_0^\infty d\omega\, \omega^3 \alpha(i\omega) f_2[\epsilon(i\omega), p], \tag{30b}$$

$$V_3(z) = Q \int_0^\infty d\omega\, \omega^3 \alpha(i\omega) f_3[\epsilon(i\omega), p]. \tag{30c}$$

For each term, one then splits the integral into two domains, $\Lambda < \hbar\omega < \infty$, and $0 < \hbar\omega < \Lambda$, where $\Lambda \sim E_h$ is a cutoff parameter. In the high-energy part $\Lambda < \hbar\omega < \infty$, one keeps the exponential suppression factor $\exp(-2\omega z/c)$, but otherwise expands the polarizability and the dielectric function for a large-frequency argument with the help of Eqs. (14) and (15). One then performs the integral over ω in the integration domain $\Lambda/\hbar < \omega < \infty$, and expands the result in powers and logarithms of z. Specifically, the logarithmic terms obtained from the high-energy part are proportional to $\ln[2\Lambda z/(\hbar c)]$. In the low-energy part $0 < \omega < \Lambda/\hbar$, one can expand the entire integrand [including the exponential suppression factor $\exp(-2\omega z/c)$] in powers of z. The condition $\omega < \Lambda/\hbar$, valid for the low-energy part together with the observation that

$$\omega \frac{z}{c} \leqslant \frac{\Lambda}{\hbar} \frac{z}{c} \ll 1, \quad z \ll \frac{a_0}{\alpha}, \quad \Lambda \sim E_h \tag{31}$$

ensures the applicability of the expansion in z of the integrand for the low-energy part. One then integrates every term obtained from the expansion of the low-energy integrand in powers of z, over the integration interval $0 < \omega < \Lambda/\hbar$. This leads to the logarithmic terms proportional to $\ln(\Lambda/E_h)$. Because Λ constitutes a scale-separation parameter, all dependence on Λ necessarily cancels at the end of the calculation when the high- and low-energy parts are added. The same mechanism lies behind the calculation of self-energy effects in hydrogenlike systems [24,25]. In view of the identity,

$$\ln\left(\frac{2\Lambda z}{\hbar c}\right) - \ln\left(\frac{\Lambda}{E_h}\right) = \ln\left(\frac{2E_h z}{\hbar c}\right) = \ln\left(\frac{2\alpha z}{a_0}\right), \tag{32}$$

the functional form of the logarithmic terms in Eq. (20) finds a natural explanation.

Applying this procedure to $V_1(z)$ as defined in Eq. (30a), one obtains the following high-energy part:

$$V_1^{\rm HEP}(\Lambda, z) = -\frac{\hbar}{16\pi^2 \epsilon_0 c^2} \frac{1}{z}\, \alpha_2\, \Omega_1 \left[\ln\left(\frac{2\Lambda z}{\hbar c}\right) + \gamma_E\right], \tag{33}$$

where we keep terms up to order $1/z$ and $\ln(z)/z$. The low-energy part can be written as

$$V_1^{\rm LEP}(\Lambda,z) = -\frac{C_{30}}{z^3} + \frac{\hbar}{16\pi^2\epsilon_0 c^2 z}\left\{\alpha_2\,\Omega_1 \ln\left(\frac{\Lambda}{E_h}\right) + \int_0^\infty d\omega\left[\alpha(i\omega)\omega^2\frac{[\epsilon(i\omega)-1][3\epsilon(i\omega)+1]}{[\epsilon(i\omega)+1]^2} - \frac{\alpha_2\,\Omega_1}{\omega+\frac{E_h}{\hbar}}\right]\right\}, \tag{34}$$

where the leading-order coefficient is

$$C_{30} = \frac{\hbar}{16\pi^2\epsilon_0}\int_0^\infty d\omega\,\alpha(i\omega)\frac{\epsilon(i\omega)-1}{\epsilon(i\omega)+1}. \tag{35}$$

The addition of the high- and low-energy parts leads to

$$V_1(z) = -\frac{C_{30}}{z^3} - \frac{\hbar}{16\pi^2\epsilon_0 c^2 z}\left\{\alpha_2\Omega_1\left[\ln\left(\frac{2E_h z}{\hbar c}\right)+\gamma_E\right] - \int_0^\infty d\omega\left[\alpha(i\omega)\omega^2\frac{[\epsilon(i\omega)-1]\,[3\epsilon(i\omega)+1]}{[\epsilon(i\omega)+1]^2} - \frac{\alpha_2\,\Omega_1}{\omega+\frac{E_h}{\hbar}}\right]\right\}, \tag{36}$$

where, again, we keep terms of orders $1/z$ and $\ln(z)/z$. We can read off the result for the logarithmic coefficient C_{11}, which multiplies the term $z^{-1}\,\ln(\frac{2E_h z}{\hbar c})$,

$$C_{11} = \frac{\hbar\,\alpha_2\,\Omega_1}{16\pi^2\epsilon_0\,c^2}. \tag{37}$$

The contribution from $V_1(z)$ to the C_{10} coefficient is

$$C_{10}^{(1)} = \frac{\hbar\gamma_E\alpha_2\Omega_1}{16\pi^2\epsilon_0 c^2} - \frac{\hbar}{16\pi^2\epsilon_0 c^2}\int_0^\infty d\omega \times\left[\alpha(i\omega)\omega^2\frac{[\epsilon(i\omega)-1][3\epsilon(i\omega)+1]}{[\epsilon(i\omega)+1]^2} - \frac{\alpha_2\Omega_1}{\omega+E_h/\hbar}\right]. \tag{38}$$

From $V_2(z)$ as defined in Eq. (30b), one obtains an additional term,

$$C_{10}^{(2)} = -\frac{\hbar\alpha_2\Omega_1}{64\pi^2\epsilon_0 c^3}. \tag{39}$$

There are no contributions from V_3 to C_{11} and C_{10}. The complete result for C_{10} reads as follows:

$$C_{10} = C_{10}^{(1)} + C_{10}^{(2)} = \frac{\hbar\left(\gamma_E-\frac{1}{4}\right)\alpha_2\,\Omega_1}{16\pi^2\epsilon_0 c^2} - \frac{\hbar}{16\pi^2\epsilon_0 c^2}\int_0^\infty d\omega \times\left[\alpha(i\omega)\omega^2\frac{[\epsilon(i\omega)-1][3\epsilon(i\omega)+1]}{[\epsilon(i\omega)+1]^2} - \frac{\alpha_2\Omega_1}{\omega+E_h/\hbar}\right]. \tag{40}$$

Quite surprisingly (see, for comparison, the case of an ideal conductor discussed in Ref. [4]), there is no coefficient on the order of $1/z^2$, and one has $C_{20}=0$, an observation which will be discussed in the following.

The same mechanism, which leads to the emergence of the logarithmic terms in z, leads to the Bethe logarithms in Lamb shift calculations [16]. At this stage, we have derived all coefficients for short range, up to the orders of $1/z$ and $\ln(z)/z$. The next step is the evaluation of the constant terms in z.

C. Higher-order coefficients

In Sec. II B, we have considered all terms in the expansion (6) up to the orders of $1/z$ and $\ln(z)/z$. We remember that the expansion (6) is valid for $z\to 0$, and, thus, an expansion in ascending powers (and logarithms) of z. In terms of the C coefficients given in Eqs. (4) and (6), we have determined the contributions to C_{11} and C_{10}, but no contributions to C_{nj} coefficients with $n=0$. Here, we list the contributions to the logarithmic coefficient C_{01} and the nonlogarithmic coefficient C_{00}, obtained from the potentials V_1, V_2, and V_3, given in Eqs. (30a), (30b), and (30c).

These higher-order coefficients, obtained from V_1, are

$$C_{01} = -\frac{\hbar\alpha_2\left(\Omega_1^2+14\Omega_2^2\right)}{96\pi^2\epsilon_0 c^3}, \tag{41}$$

$$C_{00}^{(1)} = -\frac{\hbar\alpha_2\left(7\Omega_1^2-32\Omega_2^2\right)}{288\pi^2\epsilon_0 c^3} - \frac{\gamma_E\hbar\alpha_2\left(\Omega_1^2+14\Omega_2^2\right)}{96\pi^2\epsilon_0 c^3} - \frac{\hbar}{8\pi^2\epsilon_0 c^3}\int_0^\infty d\omega\left[\frac{\alpha(i\omega)\omega^3[\epsilon(i\omega)-1]f_{00}(\epsilon(i\omega))}{24[\epsilon(i\omega)+1]^4} + \frac{7}{6}\alpha_2\Omega_1 + \frac{\alpha_2\left(\Omega_1^2+14\Omega_2^2\right)}{12(\omega+E_h/\hbar)}\right], \tag{42}$$

$$f_{00}(\epsilon) = 3\epsilon^5 - 9\epsilon^4 - 136\epsilon^3 - 208\epsilon^2 - 83\epsilon - 15. \tag{43}$$

For a dielectric function with $\Omega_1 = 0$, the coefficient C_{11} vanishes. In this case, the term proportional to C_{01} is the first nonvanishing logarithmic term in the short-range expansion of the atom-surface potential. From the potential V_2, one gets the contribution $C_{10}^{(2)}$, which had been indicated in Eq. (39), as well as the following higher-order coefficient:

$$C_{00}^{(2)} = -\frac{\hbar\alpha_2\left(\Omega_1^2+2\Omega_2^2\right)}{32\pi^2\epsilon_0 c^3}. \tag{44}$$

Furthermore, it is interesting to note that the potential $V_2(z)$ yields the only contribution to the double-logarithmic $\overline{C}_{12}$ coefficient, which multiplies the term proportional to $z\,[\ln(z)]^2$ in Eq. (6),

$$\overline{C}_{12} = -\frac{\hbar\left(4\alpha_4\Omega_1 - \alpha_2\Omega_1^3 + 4\alpha_2\Omega_1\Omega_2^2 + 4\alpha_2\Omega_3^3\right)}{64\pi^2\epsilon_0 c^4}. \tag{45}$$

Finally, from V_3, we get the following contribution to the nonlogarithmic C_{00} coefficient,

$$C_{00}^{(3)} = \frac{\hbar\alpha_2\Omega_1^2}{288\pi^2\epsilon_0 c^3}. \tag{46}$$

This concludes the discussion of the contributions to the expansion (6), from the potentials V_1, V_2, and V_3 given in Eq. (30). The potentials are obtained by expanding the function $H(\epsilon, p)$, defined in Eq. (9) for large p [see Eq. (21)].

D. Extra term

In Sec. II B, we had considered all contributions to the short-range expansion of the atom-surface potential generated by expanding the function $H(\epsilon, p)$ in powers of p for large p. After the ω integration, this expansion captures the leading terms in the (semi-)analytic expansion of $V(z)$ for $z \to 0$. However, let us remember that the expansion (21) is valid only for $p \gg 1$. The difference $H(\epsilon, p) - S(\epsilon, p)$ is nonvanishing. This difference will lead to a (parametrically suppressed) contribution to the atom-surface interaction energy from the integration interval $\omega \in (0, \infty)$ and $p \sim 1$. The only question is at which order in the expansion in ascending powers of z this additional, parametrically suppressed, contribution will become visible. This question will be answered in the current section.

In the difference term,

$$V_4(z) = \mathcal{Q} \int_0^\infty d\omega\, \omega^3 \alpha(i\omega) \int_1^\infty dp\, e^{-2\omega z p/c} \times \{H[\epsilon(i\omega), p] - S[\epsilon(i\omega), p]\}, \tag{47}$$

one can approximate $\exp(-2\omega z p/c) \approx 1$ in the limit of small z because the divergent terms in the limit of large p have already been subtracted. One can, thus, approximate $V_4(z) \approx C_{00}^{(4)}$, where

$$C_{00}^{(4)} = \frac{\hbar}{8\pi^2 \epsilon_0 c^3} \int_0^\infty d\omega\, \omega^3 \alpha(i\omega) \int_1^\infty dp \times \{H[\epsilon(i\omega), p] - S[\epsilon(i\omega), p]\}. \tag{48}$$

This completes the contributions to the nonlogarithmic coefficient C_{00}.

E. Sum of terms

Because the intricate nature of the expansion (6) and the manifold contributions to the logarithmic and nonlogarithmic coefficients, a brief summary is in order. One obtains C_{30}, C_{11}, and C_{01} exclusively from V_1 [see Eqs. (35), (37), and (41), respectively]. The coefficient C_{10} is obtained from the sum of the terms $C_{10}^{(1)}$ and $C_{10}^{(2)}$ listed in Eqs. (38) and (39). The coefficient C_{00} is obtained from the sum of the terms $C_{00}^{(1)}$, $C_{00}^{(2)}$, $C_{00}^{(3)}$, and $C_{00}^{(3)}$, listed in Eqs. (42), (44), (46), and (48). We summarize

$$C_{10} = C_{10}^{(1)} + C_{10}^{(2)}, \tag{49a}$$

$$C_{00} = C_{00}^{(1)} + C_{00}^{(2)} + C_{00}^{(3)} + C_{00}^{(4)}. \tag{49b}$$

Finally, the double logarithmic coefficient $\overline{C}_{12}$ is obtained from V_2 [see Eq. (45)].

III. NUMERICS FOR SHORT RANGE

A. Coefficients

From now on for the numerical investigations, we temporarily switch to atomic units with $\hbar = 1$, $\epsilon_0 = 1/(4\pi)$, and $c = 1/\alpha$, where α is the fine-structure constant. All energies are measured in terms of the Hartree energy $E_h = \alpha^2 mc^2$, and distances are measured in terms of the Bohr radius a_0.

It is instructive to recall all formulas for the coefficients relevant to Eq. (6), this time in atomic units. For C_{30}, one has from Eq. (35),

$$C_{30} = \frac{1}{4\pi} \int_0^\infty d\omega\, \alpha(i\omega) \frac{\epsilon(i\omega) - 1}{\epsilon(i\omega) + 1}. \tag{50}$$

For C_{11}, we scale out a factor α^2, and obtain from Eq. (37) the result,

$$\frac{C_{11}}{\alpha^2} = \frac{\alpha_2 \Omega_1}{4\pi}, \tag{51}$$

where we recall that α_2 is related to the high-frequency asymptotics of the atomic polarizability according to Eq. (14). According to the Thomas-Reiche-Kuhn sum rule [26,27], one has $\alpha_2 = N$, where N is the number of electrons in the atom. The result for the nonlogarithmic coefficient C_{10} in atomic units is relatively compact,

$$\frac{C_{10}}{\alpha^2} = \frac{\left(\gamma_E - \frac{1}{4}\right)\alpha_2 \Omega_1}{4\pi} - \int_0^\infty \frac{d\omega}{4\pi} \times \left[\alpha(i\omega)\omega^2 \frac{[\epsilon(i\omega) - 1][3\epsilon(i\omega) + 1]}{[\epsilon(i\omega) + 1]^2} - \frac{\alpha_2 \Omega_1}{\omega + 1}\right]. \tag{52}$$

For the logarithmic coefficient C_{01}, one has the following result from Eq. (41), upon conversion to atomic units,

$$\frac{C_{01}}{\alpha^3} = -\frac{\alpha_2\left(\Omega_1^2 + 14\Omega_2^2\right)}{24\pi}, \tag{53}$$

whereas the result for C_{00} in atomic units can be simplified to

$$\begin{aligned}\frac{C_{00}}{\alpha^3} = &-\frac{\alpha_2\left(15\Omega_1^2 - 14\Omega_2^2\right)}{72\pi} - \frac{\gamma_E \alpha_2\left(\Omega_1^2 + 14\Omega_2^2\right)}{24\pi} \\ &- \int_0^\infty \frac{d\omega}{2\pi} \left[\frac{\alpha(i\omega)\omega^3[\epsilon(i\omega) - 1] f_{00}[\epsilon(i\omega)]}{24[\epsilon(i\omega) + 1]^4} \right. \\ &\left. + \frac{7}{6}\alpha_2 \Omega_1 + \frac{\alpha_2\left(\Omega_1^2 + 14\Omega_2^2\right)}{12(\omega + 1)}\right] \\ &+ \int_0^\infty \frac{d\omega}{2\pi}\, \omega^3 \alpha(i\omega) \int_1^\infty dp\, [H[\epsilon(i\omega), p] \\ &- S[\epsilon(i\omega), p]],\end{aligned} \tag{54}$$

where f_{00} has been defined in Eq. (43). Finally, according to Eq. (45), the double-logarithmic coefficient $\overline{C}_{12}$ involves a scaling factor α^4 and reads as follows:

$$\frac{\overline{C}_{12}}{\alpha^4} = -\frac{4\alpha_4 \Omega_1 - \alpha_2 \Omega_1^3 + 4\alpha_2 \Omega_1 \Omega_2^2 + 4\alpha_2 \Omega_3^3}{16\pi}, \tag{55}$$

where atomic units have been employed

B. Model problem

We consider a model problem with the intent of demonstrating the power of the method described in the previous section. For definiteness and reproducibility, the coefficients of the model problem are chosen in a rather realistic manner,

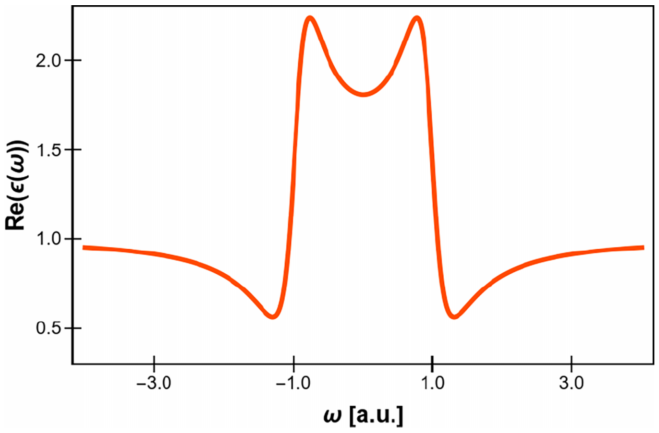

FIG. 1. The plot shows the real part of the dielectric function of the model problem defined in Eq. (56) with parameters given in Eq. (57).

leading to C_3 and C_4 coefficients, which are numerically commensurate with realistic applications, such as helium atoms interacting with silicon [14].

The model problem involves the following functional form of the dielectric function, which is inspired by the so-called Lorentz-Dirac functional form used in Ref. [14] for the description of the dielectric function of intrinsic silicon, but with only one resonance included

$$\epsilon(\omega) = 1 + \frac{\omega_p^2 - i\gamma'\omega}{\omega_0^2 - \omega^2 - i\gamma\omega}. \tag{56}$$

We choose the parameters (in atomic units),

$$\omega_0 = 1.0, \quad \omega_p = 0.9, \tag{57a}$$

$$\gamma = 0.5, \quad \gamma' = 0.2. \tag{57b}$$

The real and imaginary parts of the dielectric function of the model problem are displayed in Figs. 1 and 2, respectively. For definiteness, we calculate with the exact numerical value $\alpha = 1/137.036$ for the fine-structure constant.

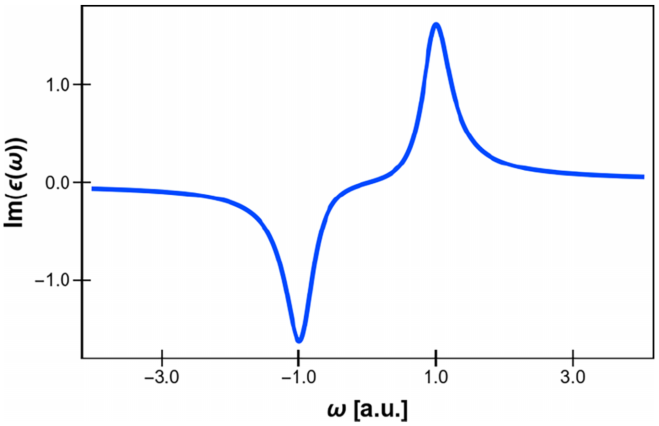

FIG. 2. The figure is the same as Fig. 1 but for the imaginary part of the dielectric function.

The dielectric function at the imaginary frequency argument reads as

$$\epsilon(i\omega) = 1 + \frac{\omega_p^2 + \gamma'\omega}{\omega_0^2 + \omega^2 + \gamma\omega}. \tag{58}$$

For the atomic polarizability, we choose the following functional form:

$$\alpha(\omega) = \frac{1}{1-\omega^2}, \quad \alpha(i\omega) = \frac{1}{1+\omega^2}, \tag{59}$$

which, for an imaginary frequency argument, approximates the trend in the data indicated in Fig. 7 of Ref. [14] for the atomic polarizability of atomic hydrogen, simultaneously providing a simple functional form.

For the model problem, one obtains the following high-frequency coefficients:

$$\alpha_2 = 1, \quad \alpha_4 = -1, \tag{60a}$$

$$\Omega_1 = \gamma' = 0.2, \tag{60b}$$

$$\Omega_2 = \left(\omega_p^2 - \gamma\gamma'\right)^{1/2} = 0.842\,615, \tag{60c}$$

$$\Omega_3 = -\left(\gamma\omega_p^2 + \gamma'\omega_0^2 - \gamma^2\gamma'^2\right)^{1/3} = -0.821\,797. \tag{60d}$$

All results are given in atomic units.

C. Expansion coefficients

One obtains the following results, where we denote the coefficients relevant to the model problem by the calligraphic symbol $\mathcal{C}$ as opposed to C, for absolute clarity:

$$\mathcal{C}_{30} = 1.977\,912\,968 \times 10^{-2}, \tag{61a}$$

$$\mathcal{C}_{11} = \alpha^2 \times 1.591\,549\,430 \times 10^{-2}, \tag{61b}$$

$$\mathcal{C}_{10} = -\alpha^2 \times 2.340\,951\,522 \times 10^{-2}, \tag{61c}$$

$$\mathcal{C}_{01} = -\alpha^3 \times 1.323\,638\,610 \times 10^{-1}, \tag{61d}$$

$$\mathcal{C}_{00} = -\alpha^3 \times 2.175\,921\,908 \times 10^{-1}, \tag{61e}$$

$$\overline{\mathcal{C}}_{12} = \alpha^4 \times 4.894\,014\,500 \times 10^{-2}. \tag{61f}$$

All results are indicated to ninr significant figures for definiteness and numerical verifiability. They use the parameters given in Sec. III B. They are given in atomic units with the appropriate power of the fine-structure constant being factored out. The calculations for the coefficient C_{00} can be somewhat involved, which is why give the contributions listed in Eqs. (42), (44), (46), and (48) separately,

$$\mathcal{C}_{00}^{(1)} = -\alpha^3 \times 1.599\,635\,302 \times 10^{-1}, \tag{62a}$$

$$\mathcal{C}_{00}^{(2)} = -\alpha^3 \times 5.809\,155\,423 \times 10^{-2}, \tag{62b}$$

$$\mathcal{C}_{00}^{(3)} = \alpha^3 \times 1.768\,388\,257 \times 10^{-4}, \tag{62c}$$

$$\mathcal{C}_{00}^{(4)} = \alpha^3 \times 2.860\,547\,387 \times 10^{-4}. \tag{62d}$$

The scaling of the higher-order coefficients with the powers of α means that the expansion is rapidly converging for not too large z, where z is expressed in atomic units, i.e., in units of the Bohr radius (see also Sec. III A).

TABLE I. For the case $z = 0.1$, the validity of the approximation (64) for the model problem discussed in Sec. III B is being verified by, subsequently, adding the $\mathcal{P}$ terms. The relative difference Δ of the partial sum of $\mathcal{P}$ terms and the exact result for $V(z = 0.1)$ is indicated in the last column. Digits displaying apparent numerical convergence are being underlined. All quantities are indicated in atomic units.

Partial sum of $\mathcal{P}$ terms	Numerical partial sum	Δ
$\mathcal{P}_{30}$	$-\underline{19.779}\,129\,681 \times 10^{-2}$	3.4×10^{-6}
$\mathcal{P}_{30} + \mathcal{P}_{11}$	$-\underline{19.779\,0}74\,340 \times 10^{-2}$	6.2×10^{-7}
$\mathcal{P}_{30} + \mathcal{P}_{11} + \mathcal{P}_{10}$	$-\underline{19.779\,061}\,874 \times 10^{-2}$	1.3×10^{-8}
$\mathcal{P}_{30} + \mathcal{P}_{11} + \mathcal{P}_{10} + \mathcal{P}_{10}$	$-\underline{19.779\,062}\,210 \times 10^{-2}$	4.2×10^{-9}
$\mathcal{P}_{30} + \mathcal{P}_{11} + \mathcal{P}_{10} + \mathcal{P}_{10} + \mathcal{P}_{00}$	$-\underline{19.779\,062\,126} \times 10^{-2}$	6.5×10^{-11}
$\mathcal{P}_{30} + \mathcal{P}_{11} + \mathcal{P}_{10} + \mathcal{P}_{10} + \mathcal{P}_{00} + \overline{\mathcal{P}}_{12}$	$-\underline{19.779\,062\,126} \times 10^{-2}$	3.5×10^{-11}
$V(z = 0.1)$ (Exact)	$-19.779\,062\,126 \times 10^{-2}$	

D. Comparison to numerical data

If our expansion (4) is the correct representation of the atom-wall interaction for $z \ll a_0/\alpha$, then the leading terms of the expansion, given in Eq. (6), should show apparent numerical convergence to the full potential, given in Eq. (8) for small values of z.

One can also write the potential $V(z)$ for the model problem in terms of individual contributions, each proportional to a particular $\mathcal{C}$ coefficient. We denote the individual terms by the symbol $\mathcal{P}$ in order to differentiate the notation from the general case, given in Eq. (5),

$$V(z) = \sum_{(n\geqslant 0)j} \mathcal{P}_{nj}(z) + \sum_{(n\leqslant 0)j} \overline{\mathcal{P}}_{nj}(z), \tag{63a}$$

$$\mathcal{P}_{nj}(z) = -\frac{\mathcal{C}_{nj}}{z^n}\left[\ln\left(\frac{2\alpha z}{a_0}\right)\right]^j, \tag{63b}$$

$$\overline{\mathcal{P}}_{nj}(z) = -\overline{\mathcal{C}}_{nj} z^n \left[\ln\left(\frac{2\alpha z}{a_0}\right)\right]^j. \tag{63c}$$

According to Eq. (6), the leading terms $\mathcal{P}_{30}$, $\mathcal{P}_{11}$, $\mathcal{P}_{10}, \mathcal{P}_{10}$ and $\mathcal{P}_{00}, \overline{\mathcal{P}}_{12}$ should exhibit numerical convergence to $V(z)$, leading to the approximation,

$$\begin{aligned} V(z) \approx{}& \mathcal{P}_{30}(z) + \mathcal{P}_{11}(z) + \mathcal{P}_{10}(z) \\ &+ \mathcal{P}_{10}(z) + \mathcal{P}_{00}(z) + \overline{\mathcal{P}}_{12}(z) \end{aligned} \tag{64}$$

for small z. We demonstrate the convergence for the case $z = 0.1$, in Table I, to about 11 decimal figures. For the case $z = 1.0$, the convergence is slower and is being demonstrated in Table II, to about seven decimal digits.

A remark is in order. Of course, the values $z = 0.1$ as well as $z = 1.0$ represent situations in which the atom is too close to the surface for the atom-surface potential to be physically applicable. For $z = 0.1$, one would have a situation with the atomic wave functions overlapping with the wall; the case of $z = 0.1$ is presented for numerical completion. The significance of the numerical data given in Tables I and II is that they indicate the consistency of our (semi-)analytic expansion of the atom-surface potential for short range with high numerical precision, including the existence of the logarithmic terms. This offers an excellent way to illustrate the convergence of the short-range expansion (6).

The terms in Eq. (6) display a definitive hierarchy: For short range ($z \to 0$), the logarithms are enhanced, and terms are suppressed in ascending powers of z, i.e., terms proportional to $1/z^3$ dominate terms of order $1/z$, and so on. We define the following two remainder functions $r_{nj}(z)$ in terms of the remainder term left over after adding the all terms of lower order than $P_{nj}(z)$. In atomic units, one has the following relations:

$$r_{10}(z) = \frac{z}{\alpha^2}\left[V(z) + \frac{\mathcal{C}_{30}}{z^3} + \frac{\mathcal{C}_{11}}{z}\ln(2\alpha z)\right], \tag{65}$$

$$\begin{aligned} r_{00}(z) = \frac{1}{\alpha^3}\Bigg[& V(z) + \frac{\mathcal{C}_{30}}{z^3} + \frac{\mathcal{C}_{11}}{z}\ln(2\alpha z) + \frac{\mathcal{C}_{10}}{z} \\ &+ \mathcal{C}_{01}\ln(2\alpha z) + \overline{\mathcal{C}}_{12} z \ln^2(2\alpha z)\Bigg] \end{aligned} \tag{66}$$

If our expansion (6) is correct, then we should obtain the results that

$$\lim_{z\to 0} r_{10}(z) = \frac{\mathcal{C}_{10}}{\alpha^2} = -0.023\,409. \tag{67}$$

$$\lim_{z\to 0} r_{00}(z) = \frac{\mathcal{C}_{00}}{\alpha^3} = -0.021\,759. \tag{68}$$

TABLE II. We present the analog of Table I for the case $z = 1.0$.

Partial sum of $\mathcal{P}$ terms	Numerical partial sum	Δ
$\mathcal{P}_{30}$	$-\underline{1.977}\,912\,97 \times 10^{-2}$	2.3×10^{-3}
$\mathcal{P}_{30} + \mathcal{P}_{11}$	$-\underline{1.977}\,554\,71 \times 10^{-2}$	5.6×10^{-3}
$\mathcal{P}_{30} + \mathcal{P}_{11} + \mathcal{P}_{10}$	$-\underline{1.977\,4}30\,05 \times 10^{-2}$	7.1×10^{-6}
$\mathcal{P}_{30} + \mathcal{P}_{11} + \mathcal{P}_{10} + \mathcal{P}_{10}$	$-\underline{1.977\,4}51\,79 \times 10^{-2}$	3.9×10^{-6}
$\mathcal{P}_{30} + \mathcal{P}_{11} + \mathcal{P}_{10} + \mathcal{P}_{10} + \mathcal{P}_{00}$	$-\underline{1.977\,443}\,34 \times 10^{-2}$	3.7×10^{-7}
$\mathcal{P}_{30} + \mathcal{P}_{11} + \mathcal{P}_{10} + \mathcal{P}_{10} + \mathcal{P}_{00} + \overline{\mathcal{P}}_{12}$	$-\underline{1.977\,443}\,58 \times 10^{-2}$	2.5×10^{-7}
$V(z = 0.1)$ (Exact)	$-1.977\,444\,07 \times 10^{-2}$	

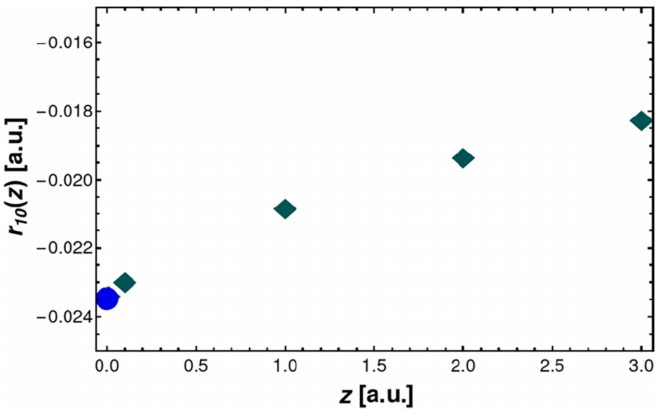

FIG. 3. Numerical data for the function $r_{10}(z)$ defined in Eq. (67) (diamonds) are plotted for short-range z values and compared to the limit $\lim_{z\to 0} r_{10}(z) = C_{10}/\alpha^2 = -0.023\,409$ (circle).

The numerical data presented in Figs. 3 and 4 are consistent with Eqs. (67) and (68).

IV. LONG-RANGE ASYMPTOTICS

A. General considerations

Now, we switch back to SI mksA units and look at the long-range limit $z \gg a_0$ for the atom-surface interaction potential $V(z)$. For convenience, we recall Eq. (8) in the form

$$V(z) = -\frac{\hbar}{8\pi^2\epsilon_0 c^3}\int_0^\infty d\omega\,\omega^3\alpha(i\omega) \times \int_1^\infty dp\,H(\epsilon(i\omega),p)e^{-2p\omega z/c}, \tag{69}$$

aiming to expand for large z where the exponential suppression due to the term $e^{-2p\omega z/c}$ is very pronounced. The relevant integration interval for the virtual photon energy, therefore, encompasses low frequencies on the atomic scale $\omega \ll E_h/\hbar$. For the p integration, we can concentrate on the integration region near $p = 1$ due to exponential suppression. One can, thus, expand both the atomic polarizability as well as the dielectric function for small frequency arguments. For the atomic polarizability, this implies that

$$\alpha(i\omega) = \alpha(i\omega) + i\omega\alpha'(0) - \frac{\omega^2}{2}\alpha''(0) + O(\omega^3), \tag{70}$$

and

$$H(\epsilon(i\omega),p) = H(\epsilon(0),p) + \omega\left(\left.\frac{\partial H(\epsilon,p)}{\partial\epsilon}\right|_{\epsilon=\epsilon(0)}\right) \times \left(i\left.\frac{\partial\epsilon(\omega)}{\partial\omega}\right|_{\omega=0}\right) + O(\omega^2). \tag{71}$$

The quantities,

$$\mathcal{T}_1 = i\omega\alpha'(0), \quad \mathcal{T}_2 = \left(i\left.\frac{\partial\epsilon(\omega)}{\partial\omega}\right|_{\omega=0}\right) \tag{72}$$

are, surprisingly, real rather than complex. In order to see this, we consider the fact that the first derivatives of the polarizability and the dielectric function are generated by the small "width terms" in the propagator denominators. We recall the H function from Eq. (9),

$$H(\epsilon,p) = \frac{s-p}{s+p} + (1-2p^2)\frac{s-p\epsilon}{s+p\epsilon}, \quad s = \sqrt{\epsilon-1+p^2}. \tag{73}$$

Some properties of the H function and of its derivatives are of interest. We have

$$H(\epsilon,p=1) = \frac{2(\sqrt{\epsilon}-1)}{\sqrt{\epsilon}+1}, \quad H(\epsilon,p\to\infty) = \frac{2(\epsilon-1)}{\epsilon+1}p^2. \tag{74}$$

In view of the expansion (71), it is necessary to consider the derivative of the H function with respect to the first argument ϵ, and to make sure that its derivatives do not diverge stronger than p^2 because of possible infrared problems in the ω integral generated by divergences (high negative powers of ω after the p integration). Or, expressed differently, if we carry out the ω integral first, then we observe that

$$\int_0^\infty d\omega\,\omega^3\alpha(i\omega)e^{-2p\omega z/c} \approx \frac{3c^4\alpha(0)}{8\,p^4\,z^4}. \tag{75}$$

Any divergence of H or of its derivatives stronger than p^2 would make the p integral divergent at the upper limit because it would multiply a term proportional to $1/p^4$. We will evaluate both at the lower limit $p = 1$ of the integration range over p as well as the upper limit $p = \infty$. For the first and second derivatives, we have

$$\left.\frac{\partial H(\epsilon,p)}{\partial\epsilon}\right|_{p=1} = \frac{2}{\sqrt{\epsilon}(\sqrt{\epsilon}+1)^2}, \tag{76}$$

$$\left.\frac{\partial H(\epsilon,p)}{\partial\epsilon}\right|_{p\to\infty} = \frac{4}{(\epsilon+1)^2}p^2, \tag{77}$$

$$\left.\frac{\partial^2 H(\epsilon,p)}{\partial\epsilon^2}\right|_{p=1} = -\frac{3\sqrt{\epsilon}+1}{\epsilon^{3/2}(\sqrt{\epsilon}+1)^3}, \tag{78}$$

$$\left.\frac{\partial^2 H(\epsilon,p)}{\partial\epsilon^2}\right|_{p\to\infty} = -\frac{8}{(\epsilon+1)^3}p^2. \tag{79}$$

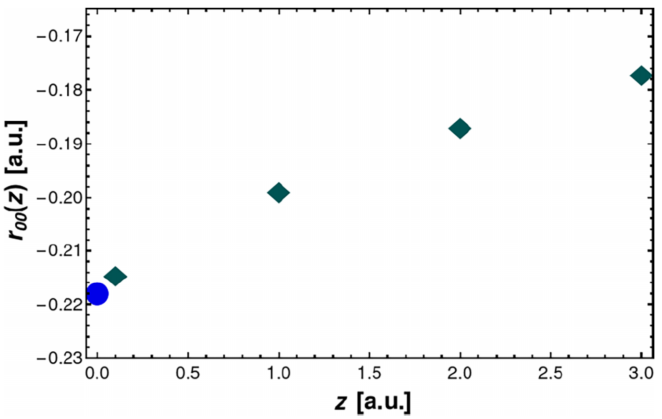

FIG. 4. Numerical data for the function $r_{00}(z)$ defined in Eq. (68) (diamonds) are plotted for short-range z values and compared to the limit $\lim_{z\to 0} r_{00}(z) = C_{00}/\alpha^2 = -0.021\,759$ (circle).

At $p = \infty$, the second derivative of the H function does not diverge stronger than p^2.

B. Expansion for long range

In view of the considerations reported in Sec. IV A, we can ascertain that the long-range expansion of the atom-wall potential is

$$V(z) = -\frac{C_4}{z^4} - \frac{C_5}{z^5} - \frac{C_6}{z^6} + O(z^{-7}), \tag{80}$$

without the presence of any logarithmic terms. The leading coefficient C_4 is obtained as follows:

$$C_4 = \frac{3c\hbar\alpha(0)}{32\pi^2\epsilon_0 z^4}\Psi(\epsilon(0)). \tag{81}$$

Here, $\Psi(\epsilon)$ is a function which is normalized to unity in the limit $\epsilon(0) \to \infty$ (limit of a perfect conductor) and which can otherwise be expressed as follows:

$$\Psi(\epsilon) = A(\epsilon) + B(\epsilon)\ln\left(\frac{\sqrt{\epsilon-1}-\sqrt{\epsilon}+1}{\sqrt{\epsilon-1}+\sqrt{\epsilon}-1}\right) + C(\epsilon)\ln\left(\frac{\sqrt{\epsilon+1}-\sqrt{\epsilon}+1}{\sqrt{\epsilon+1}+\sqrt{\epsilon}-1}\right). \tag{82}$$

An alternative representation of the Ψ function (with a different normalization factor) has been given in Eq. (23) of Ref. [13]. We here aim to express Ψ in a slightly more concise form as compared to Eq. (23) of Ref. [13], namely, with the help of only two logarithmic terms. The coefficients involve both fractional and integer powers of ϵ,

$$A(\epsilon) = \frac{6\epsilon^2 - 3\epsilon^{3/2} - 4\epsilon - 3\sqrt{\epsilon} + 10}{6(\epsilon-1)}, \tag{83a}$$

$$B(\epsilon) = \frac{2\epsilon^3 - 4\epsilon^2 + 3\epsilon + 1}{2(\epsilon-1)^{3/2}}, \tag{83b}$$

$$C(\epsilon) = -\frac{\epsilon^2}{\sqrt{\epsilon+1}}. \tag{83c}$$

The first two correction terms about the perfect-conductor limit lead to the following expansion for the C_4 coefficient:

$$C_4 = \frac{3\hbar c\alpha(0)}{32\pi^2\epsilon_0}\left[1 - \frac{5}{4\sqrt{\epsilon(0)}} + \frac{22}{15\epsilon(0)} + O\left(\frac{1}{\epsilon(0)^{3/2}}\right)\right]. \tag{84}$$

By expanding the integrand as in Eq. (70), one obtains the C_5 coefficient as follows:

$$C_5 = \frac{3\hbar c^2}{32\pi^2\epsilon_0}[-i\alpha'(0)]\Psi^{(5)}(\alpha,\epsilon), \tag{85}$$

where we take note of the fact that $\alpha'(0)$ is imaginary. Here,

$$\Psi^{(5)}(\alpha,\epsilon) = -\frac{i\alpha(0)}{\alpha'(0)}\int_1^\infty \frac{dp}{p^5}\left[H(\epsilon(0),p)\frac{i\alpha'(0)}{\alpha'(0)} + \left(\frac{\partial H(\epsilon,p)}{\partial\epsilon}\bigg|_{\epsilon=\epsilon(0)}\right)\left(i\frac{\partial\epsilon(\omega)}{\partial\omega}\bigg|_{\omega=0}\right)\right]. \tag{86}$$

This integral converges both at the lower as well as the upper limit. The perfect conductor limit is

$$\Psi^{(5)}(\alpha,\epsilon) = 1 + O\left(\frac{1}{\sqrt{\epsilon(0)}}\right). \tag{87}$$

For the term C_6, one finds

$$C_6 = \frac{15\hbar c^3}{64\pi^2\epsilon_0}\alpha''(0)\Psi^{(6)}(\alpha,\epsilon), \tag{88}$$

where the coefficient ϕ_6 is given as

$$\begin{aligned}\Psi^{(6)}(\alpha,\epsilon) &= -\frac{\alpha(0)}{2\alpha''(0)}\int_1^\infty \frac{dp}{p^6}\left[H[\epsilon(0),p]\frac{\alpha''(0)}{\alpha(0)}\right. \\ &+ \left(\frac{\partial^2 H(\epsilon,p)}{\partial\epsilon^2}\bigg|_{\epsilon=\epsilon(0)}\right)\left(\frac{\partial\epsilon(\omega)}{\partial\omega}\bigg|_{\omega=0}\right)^2 \\ &+ \left\{2\frac{\alpha'(0)}{\alpha(0)}\left(\frac{\partial\epsilon(\omega)}{\partial\omega}\bigg|_{\omega=0}\right) + \left(\frac{\partial^2\epsilon(\omega)}{\partial\omega^2}\bigg|_{\omega=0}\right)\right\} \\ &\left.\times\left(\frac{\partial H(\epsilon,p)}{\partial\epsilon}\bigg|_{\epsilon=\epsilon(0)}\right)\right].\end{aligned} \tag{89}$$

Again, all integrals converge, and the perfect-conductor limit is

$$\Psi^{(6)}(\alpha,\epsilon) = 1 + O\left(\frac{1}{\sqrt{\epsilon(0)}}\right). \tag{90}$$

Now, we turn our attention to a numerical example.

V. NUMERICS FOR LONG RANGE

A. Expansion coefficients

For the numerical calculations, just as in Sec. III A, let us write the relevant coefficients given in Eqs. (81), (85), and (88) in atomic units. They read as follows:

$$C_4 = \frac{3}{8\pi\alpha}\alpha(0)\Psi(\epsilon(0)), \tag{91a}$$

$$C_5 = \frac{3}{8\pi\alpha^2}[-i\alpha'(0)]\Psi^{(5)}(\alpha,\epsilon), \tag{91b}$$

$$C_6 = \frac{15}{16\pi\alpha^3}\alpha''(0)\Psi^{(6)}(\alpha,\epsilon). \tag{91c}$$

For the model problem discussed in Sec. III B, the results are as follows:

$$\mathcal{C}_4 = \alpha^{-1} \times 2.617\,284\,022 \times 10^{-2}, \tag{92a}$$

$$\mathcal{C}_5 = -\alpha^{-2} \times 4.126\,588\,852 \times 10^{-3}, \tag{92b}$$

$$\mathcal{C}_6 = -\alpha^{-3} \times 5.762\,148\,081 \times 10^{-2}. \tag{92c}$$

Parametrically, in atomic units, the higher-order terms acquire another power of α with each order in the expansion in $1/z$.

TABLE III. For the case of $z = 100\,00.0$, the approximation (93) is investigated for the model problem discussed in Sec. III B, by, subsequently, adding the $\mathcal{P}$ terms. The relative difference Δ of the partial sum of $\mathcal{P}$ terms and the exact result for $V(z = 100\,00.0)$ is indicated in the last column. Digits displaying apparent numerical convergence are being underlined. All quantities are indicated in atomic units.

Partial sum of $\mathcal{P}$ terms	Numerical value	Δ
$\mathcal{P}_4$	$-\underline{3.586}\,621 \times 10^{-10}$	2.6×10^{-3}
$\mathcal{P}_4 + \mathcal{P}_5$	$-\underline{3.578}\,872 \times 10^{-10}$	4.1×10^{-4}
$\mathcal{P}_4 + \mathcal{P}_5 + \mathcal{P}_6$	$-\underline{3.577}\,389 \times 10^{-10}$	5.0×10^{-6}
$V(z = 10000.0)$ (Exact)	$-3.577\,407 \times 10^{-10}$	

This means that the expansion parameter, effectively, is αz, For the case of $z = 10\,000$ (which implies $\alpha z = 72.9735$), the validity of the approximation,

$$V(z) \approx \mathcal{P}_4(z) + \mathcal{P}_5(z) + \mathcal{P}_6(z) \approx -\frac{\mathcal{C}_4}{z^4} - \frac{\mathcal{C}_5}{z^5} - \frac{\mathcal{C}_6}{z^6}, \tag{93}$$

with an obvious definition of $\mathcal{P}_4(z)$, $\mathcal{P}_5(z)$, and $\mathcal{P}_6(z)$, is being demonstrated in Table III.

B. Comparison to numerical data

Some general remarks on applicable approximations to the atom-surface potential are in order. Namely, our considerations for the short-range regime clearly indicate the presence of logarithmic terms, which are not captured in the simple interpolating formula given in Eq. (3). In fact, one particular deficiency of Eq. (3) is that upon expansion for small z, a term on the order of $1/z^2$ is being generated, which is not present in Eq. (6).

For the model problem defined in Sec. III B, the leading terms in the short-range expansions are

$$V(z) \approx -\frac{\mathcal{C}_{30}}{z^3}, \quad z \ll \frac{a_0}{\alpha}, \tag{94}$$

In the long-range regime, one has

$$V(z) \approx -\frac{\mathcal{C}_4}{z^4}, \quad z \gg \frac{a_0}{\alpha}. \tag{95}$$

We investigate the interpolating regime $z \sim a_0/\alpha$ in Fig. 5 and confirm the transition between the short-range ($\propto 1/z^3$) and long-range ($\propto 1/z^4$) asymptotics of the atom-surface potential.

The rational approximation for $V(z)$ given in Eq. (3) can be adapted to the model problem discussed in Sec. III B,

$$V_r(z) \approx \frac{\mathcal{C}_4}{z^3(z + L)}, \quad L = \frac{\mathcal{C}_4}{\mathcal{C}_{30}}, \tag{96}$$

In Fig. 6, we present data for the function,

$$\chi(z) = \left| \frac{V_r(z) - V(z)}{V(z)} \right|, \tag{97}$$

which is the relative difference of the full potential and the rational approximation. We find a 20% deviation in the intermediate region $z \sim a_0/\alpha$, consistent with the inadequacy of the rational interpolation (3).

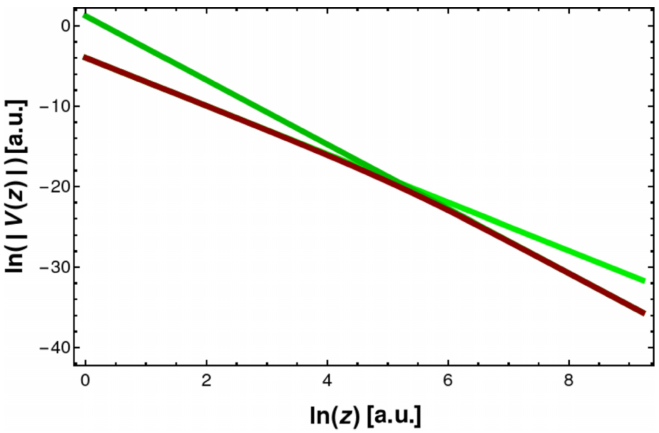

FIG. 5. The transition from the short-range $1/z^3$ to the long-range $1/z^4$ regime [see Eqs. (94) and (95)] (green curves) is being demonstrated by comparison to the full potential (red curve) given in Eq. (8). The change in the slope of the red curve in the transition region is clearly visible in the double-logarithmic plot.

Of course, it is possible to designate other methods for the fitting of the full potential $V(z)$ in the intermediate region $z \sim a_0/\alpha$, for example, by using the short-range expansion for $z \lesssim 30$, the long-range expansion for $z \gtrsim 1000$, and fitting the logarithm of the interaction potential in the intermediate region using convenient functional forms. Corresponding results will be presented elsewhere. However, our findings indicate that the presence of logarithms in the short-range expansion cannot be ignored, a fact, which fundamentally alters our understanding of the functional form of the atom-surface potential for close approach.

VI. CONCLUSIONS

Let us briefly summarize the findings of the current investigation. In Sec. I, we have discussed possible functional forms for the interpolation between the known short-range and long-range asymptotics limits of the atom-surface potential [see Eqs. (1)–(3)]. The derivation of the leading short-range logarithmic and nonlogarithmic coefficients $\mathcal{C}_{30}$, $\mathcal{C}_{11}$, and $\mathcal{C}_{10}$ for a realistic dielectric function has been discussed in Sec. II. In Sec. III, the existence of the logarithmic terms, involving logarithms of the functional form $\ln(2\alpha z)$ (in atomic units) has been demonstrated on the basis of numerical calculations. In Sec. IV, the derivation of the long-range expansion has proceeded accordingly with only nonlogarithmic terms found. In Sec. V, a comparison to numerical data for long range has been indicated, and the failure of the simple interpolating form (96) has been demonstrated in Fig. 6. We can confirm that the same phenomenon (failure of simple rational approximations in the interpolating region) is being observed for nonmodel problems, such as helium interacting with a silicon surface [14]; detailed results will be presented elsewhere. The model problem discussed in Sec. III B has all characteristics expected for atoms interacting with a dielectric surface, while simultaneously, providing a sufficiently simple functional form to make independent verifications of the findings reported in this paper easily possible.

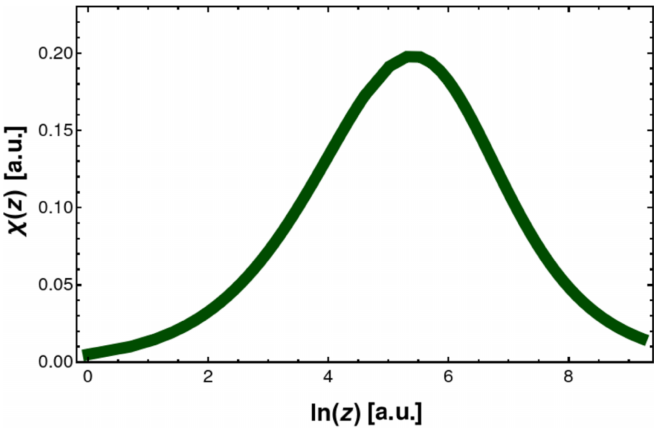

FIG. 6. We show the relative difference of the rational approximation and the exact potential, as parametrized by the function $\chi(z)$ defined in Eq. (97). In the intermediate region, one has a difference of about 20%.

Atom-wall potentials are needed as input for other calculations, such as quantum reflection off surfaces [5,6], and it is advantageous to have a compact analytic form of the atom-wall potential available without having to resort to numerical integration for each and every given z [see Eq. (8)]. In this context, it is especially useful to know why interpolating rational approximations are not adequate in intermediate regions of the atom-wall distance, and why, in particular, no term of order $1/z^2$ is present in the short-range expansion for a realistic dielectric function. The emergence of the logarithmic terms is especially important for cases where the dielectric function is described by complex oscillator strengths, which result in a nonvanishing coefficient Ω_1 in Eq. (19) and a nonvanishing C_{11} coefficient as given in Eq. (37).

Indeed, for interactions with a realistic dielectric surface, we have shown that no term of order $1/z^2$ exists in the short-range expansion [see Eq. (6)]. However, in order to put this finding into proper context, we show, in Appendix A, that the limit of a perfect conductor is approached nonuniformly in terms of the functional form of the short-range expansion: Namely, for an absolutely perfect conductor, there actually is a term proportional to $1/z^2$ present (see Appendix A). However, for any realistic dielectric, the approximation $\epsilon(i\omega) \approx \infty$ breaks down at a sufficiently high angular frequency ω, and the coefficient of order $1/z^2$ vanishes, via the mechanism described in Appendix A.

One might wonder about the naturalness of the emergence of the logarithmic terms from the integral representation of the atom-surface potential. Hence, some remarks are in order. In Appendix B, we aim to illustrate the emergence of the logarithmic terms on the basis of a model integral, which can otherwise be expressed in terms of exponential integrals. Still, the logarithmic terms emerge from the addition of the high-energy and low-energy parts.

Finally, we include some remarks on an interesting phenomenon of "confluence" in the transition range of $z \sim a_0/\alpha$. Namely, all terms in the short-range expansion (6), and all terms in the long-range expansion (7), assume the same order of magnitude,

$$V(z) \sim \alpha^5 mc^2, \qquad z \sim \frac{a_0}{\alpha}, \tag{98}$$

which is the same order of magnitude that is obtained for the Lamb-shift corrections in hydrogenlike systems [17], which is the same order of magnitude as the Bethe-logarithm correction for hydrogen energy levels [16]. Indeed, we observe the confluence of the short-range expansion (6), and long-range expansion (7) at the scale $z \sim 137\, a_0$, and its correspondence with the scale of the Bethe logarithm. Furthermore, we observe the analogy of the short-range expansion (6) with the semianalytic expansion of the Lamb shift (see Refs. [28] and Chap. 15 of [17]) where, in the latter case, one encounters logarithmic terms of the form $\ln[(Z\alpha)^{-2}]$, where Z is the nuclear charge number. The Bethe logarithm can be written as an integral over a matrix element of the reference state [17], which resembles the polarizability $\alpha(\omega)$ but is restricted to virtual photon creation processes. The integral defining the Bethe logarithm can be written as a logarithmic sum over dipole transition elements to virtual states and sums over logarithms of excitation energies [16]. The same is true for the short-range coefficients C_{10} and C_{00} from Eq. (6). Hence, it is a natural identification to refer to the coefficients C_{10} and C_{00} as "interactive Bethe logarithms."

ACKNOWLEDGMENT

Support from the National Science Foundation (Grant No. PHY–2110294) is gratefully acknowledged.

APPENDIX A: NONUNIFORM LIMIT OF PERFECT CONDUCTOR

The limit of a perfect conductor ($\epsilon \to \infty$) of Eq. (8) has been derived in Ref. [4] as follows:

$$V(z) = -\int_0^\infty \frac{d\omega\, \hbar\alpha(i\omega)}{(4\pi)^2\epsilon_0 z^3}\left[1 + \frac{2\omega z}{c} + 2\left(\frac{\omega z}{c}\right)^2\right] e^{-2\omega z/c}. \tag{A1}$$

The following expansion has been derived in Ref. [4] for a perfect conductor,

$$V(z) = -\frac{\hbar}{(4\pi)^2\epsilon_0 z^3}\int_0^\infty d\omega\, \alpha(i\omega) + \frac{3\alpha}{4\pi} N\alpha^2 mc^2 \left(\frac{a_0}{z}\right)^2 + O(z^{-1}). \tag{A2}$$

Here, N is the number of electrons.

One might now ask why the expansion (6) has a vanishing coefficient on the order of $1/z^2$ (nonlogarithmic term), whereas, the coefficient on the order of $1/z^2$ in Eq. (A2) is manifestly nonvanishing. In order to understand the phenomenon, let us consider the f_1 function from Eq. (24),

$$f_1(\epsilon, \omega) \approx e^{-2\omega z/c}\left[\frac{1}{2}\left(\frac{c}{\omega z}\right)^3 + \left(\frac{c}{\omega z}\right)^2\right]\frac{\epsilon - 1}{\epsilon + 1} \tag{A3}$$

If we can expand the term proportional to $z^{-3}e^{-2\omega z/c}$ in powers of z, the term on the orde of $1/z^2$ vanishes for any possible ϵ. The crucial observation is that this expansion is forbidden for a perfect conductor because it leads to a divergent integral over ω. Namely, for a realistic material and large ω, one has

the following relation according to Eq. (15):

$$\frac{\epsilon(i\omega)-1}{\epsilon(i\omega)+1}=\frac{\Omega_1}{2\omega}+O\left(\frac{1}{\omega^2}\right), \tag{A4}$$

whereas, for a perfect conductor, one has

$$\frac{\epsilon(i\omega)-1}{\epsilon(i\omega)+1}\to 1, \quad \epsilon(i\omega)\to\infty. \tag{A5}$$

The polarizability at the imaginary frequency argument has the asymptotics given in Eq. (14). Considering the expression,

$$X(\omega)=\omega\alpha(i\omega)\frac{\epsilon(i\omega)-1}{\epsilon(i\omega)+1}=\frac{\alpha_2\Omega_1}{2\omega^2}+O(\omega^{-3}), \tag{A6}$$

we see that its integral over ω converges at the upper limit of integration for a realistic material in the limit $\omega\to\infty$. However, for a perfect conductor, one has

$$X(\omega)=\omega\alpha(i\omega)\frac{\epsilon(i\omega)-1}{\epsilon(i\omega)+1}=\frac{\alpha_2}{\omega}+O(\omega^{-2}), \tag{A7}$$

and, therefore, the integral of $X(\omega)$ over ω diverges for large ω. So, we cannot approach the limit of a perfect conductor uniformly. Conversely, for a perfect conductor, we cannot expand the exponential in the integrand in Eq. (8) to first subleading order in z, and we also cannot expand the exponential in Eq. (A3) to first order in z without giving rise to a divergent integral over ω. We conclude that the term on thr order of $1/z^2$ in Eq. (A2), being proportional to the number of electrons of the atom, is spurious and a consequence of the physically nonsensical assumption of an infinite dielectric function of the perfect conductor over all frequency ranges; this assumption breaks down in the limit of large ω, and this region is decisive for the presence or lack of the $1/z^2$ coefficient.

APPENDIX B: OVERLAPPING PARAMETER

The method of the overlapping parameter is the decisive ingredient in the derivation of the logarithmic terms in Eq. (6). Here, we consider a model problem to illustrate the method. The model problem consists of the integral,

$$F(z)=\int_0^\infty d\omega\,\exp\left(-\frac{z\omega}{c}\right)\frac{\omega}{\omega^2+(2E_h/\hbar)^2} \tag{B1}$$

for which we aim to find a short-range (small z) expansion. After a partial fraction decomposition of the expression $\omega/[\omega^2+(2E_h/\hbar)^2]$, one can express the integral $F(z)$ in terms of exponential integral functions. Applicable expansions in powers and logarithms of z can be found in reference works [29].

However, that calculation is not our goal, here, since we are aiming at illustrating the method of the overlapping parameter. We, thus, separate the integral into a low-energy part, and a high-energy part where the high-energy part comprises the interval $\Lambda/\hbar<\omega<0$, and the low-energy part comprises the interval $0<\omega<\Lambda/\hbar$. We have

$$F(z)=F_{\rm HEP}(\Lambda,z)+F_{\rm LEP}(\Lambda,z), \tag{B2}$$

$$F_{\rm HEP}(\Lambda,z)=\int_{\Lambda/\hbar}^\infty d\omega\,\exp\left(-\frac{z\omega}{c}\right)\frac{\omega}{\omega^2+(2E_h/\hbar)^2}, \tag{B3}$$

$$F_{\rm LEP}(\Lambda,z)=\int_0^{\Lambda/\hbar} d\omega\,\exp\left(-\frac{z\omega}{c}\right)\frac{\omega}{\omega^2+(2E_h/\hbar)^2}. \tag{B4}$$

The idea is to expand both parts in z for small z. Subsequently, every term obtained in the expansion for small z is separately expanded for large Λ. The divergent terms (in Λ) should cancel in the sum $F(z)$. Finally, $F(z)$ can be expressed as a semianalytic expansion in powers of z and $\ln(z)$.

The expansion in z is accomplished as follows:

$$F_{\rm HEP}(\Lambda,z)=\int_{\Lambda/\hbar}^\infty d\omega\,e^{-z\omega/c}\underbrace{\frac{\omega}{\omega^2+(2E_h/\hbar)^2}}_{\text{expand for large }\omega}, \tag{B5}$$

$$F_{\rm LEP}(\Lambda,z)=\int_0^{\Lambda/\hbar}\frac{d\omega\,\omega}{\omega^2+(2E_h/\hbar)^2}\underbrace{\exp\left(-\frac{z\omega}{c}\right)}_{\text{expand in }z}. \tag{B6}$$

For the high-energy part, one expands the expression $\omega/[\omega^2+(2E_h/\hbar)^2]$ in ω for large ω, integrates over ω, then expands in powers of z, and then, one expands in Λ for large Λ (in that sequence). For the low-energy part, one expands the integrand in powers of z, then integrates over ω, and then, one expands in Λ for large Λ (in that sequence). The results of these procedures are as follows:

$$F_{\rm HEP}(\Lambda,z)=-\ln\left(\frac{\Lambda z}{\hbar c}\right)+\frac{\Lambda z}{\hbar c}-\gamma_E+z^2\left[-\frac{\Lambda^2}{4\hbar^2c^2}+\frac{E_h^2}{2\hbar^2c^2}\ln\left(\frac{\Lambda z}{\hbar c}\right)+\gamma_E\frac{E_h^2}{2\hbar^2c^2}-\frac{3E_h^2}{4\hbar^2c^2}\right], \tag{B7}$$

$$F_{\rm LEP}(\Lambda,z)=\ln\left(\frac{\Lambda}{2E_h}\right)+z\left(-\frac{\Lambda}{\hbar c}+\frac{\pi E_h}{\hbar c}\right)+z^2\left[\frac{\Lambda^2}{4\hbar^2c^2}-\frac{2E_h^2}{\hbar^2c^2}\ln\left(\frac{\Lambda}{2E_h}\right)\right], \tag{B8}$$

where higher-order terms of orders z^3 and $z^3\ln(z)$ are ignored. The sum of the high- and low-energy parts is

$$F(z)=-\ln\left(\frac{2E_hz}{\hbar c}\right)-\gamma_E+\pi\frac{E_hz}{\hbar c}+\left(\frac{E_hz}{\hbar c}\right)^2\left[2\ln\left(\frac{2E_hz}{\hbar c}\right)+2\gamma_E-3\right]. \tag{B9}$$

We see that Λ has canceled as promised, and logarithmic terms have appeared.

Let us now discuss the physically reasonable range for Λ. One assumes that z is on the same order as the Bohr radius, and that the cutoff parameter Λ is on the order of E_h/α,

$$z\sim a_0. \tag{B10}$$

In the low-energy part, one must still be allowed to expand the exponential $\exp(-z\omega/c)$ in the argument $z\omega/c$. So, we must have

$$\frac{z\omega}{c}\lesssim 1, \quad \omega\lesssim\frac{\Lambda}{\hbar}, \tag{B11}$$

where the latter condition is due to the upper integration limit of the low-energy part. If we use the assumption $z\sim a_0$ and the value of $\omega=\Lambda/\hbar$ in the first inequality, then we obtain the condition,

$$\frac{a_0\Lambda}{\hbar c}\lesssim 1. \tag{B12}$$

The resulting condition on Λ is that

$$\Lambda \lesssim \frac{\hbar c}{a_0} = \frac{E_h}{\alpha}. \tag{B13}$$

This result confirms that an appropriate order of magnitude for the cutoff parameter Λ is E_h/α. Conversely, the expansion of the quantity $[\omega/(\omega^2 + (2E_h/\hbar)^2)]$ for large ω is possible when we have $\hbar\omega \gg E_h$. That this condition is fulfilled, follows from the fact that $\Lambda \sim E_h/\alpha$ and, thus, $\hbar\omega \geqslant \Lambda \sim E_h/\alpha \gg E_h$.

Let us also discuss the extraction of the finite part of the low-energy part. For the lowest-order term in the expansion in z, one replaces $\exp(-\frac{z\omega}{c}) \to 1$ in the integrand and writes

$$F_{\rm LEP}(\Lambda, z) \approx L \equiv \int_0^{\Lambda/\hbar} d\omega \frac{\omega}{\omega^2 + (2E_h/\hbar)^2}. \tag{B14}$$

The finite part of the integral can be found as follows. One first expands the integrand $\omega/[\omega^2 + (2E_h/\hbar)^2]$ for large ω, to find the divergent terms for large Λ, and then, one replaces $1/\omega \to 1/(\omega + E_h/\hbar)$, in order to avoid infrared divergences. The result is

$$L = \int_0^{\Lambda/\hbar} d\omega \frac{\omega}{\omega^2 + (2E_h/\hbar)^2} = \int_0^{\Lambda/\hbar} d\omega \frac{1}{\omega + E_h/\hbar} + J,$$
$$J = \int_0^{\infty} d\omega \left[\frac{\omega}{\omega^2 + (2E_h/\hbar)^2} - \frac{1}{\omega + E_h/\hbar}\right] = -\ln(2). \tag{B15}$$

In the second ultraviolet convergent term, one can let $\Lambda \to \infty$. So, one finds the result,

$$L = \ln\left(\frac{\Lambda + E_h}{E_h}\right) + J = \ln\left(\frac{\Lambda}{E_h}\right) - \ln(2) + O(\Lambda^{-1}). \tag{B16}$$

Analogous procedures are employed in the calculations of the logarithmic and nonlogarithmic terms for the atom-wall interaction.

[1] *Casimir Physics*, Lecture Notes in Physics, edited by D. Dalvit, P. Milonni, D. Roberts, and F. de Rosa (Springer, Heidelberg, 2011), Vol. 834.

[2] E. M. Lifshitz, The theory of molecular attractive forces between solids, Zh. Éksp. Teor. Fiz. **29**, 94 (1955) [Sov. Phys. JETP **2**, 73 (1956)].

[3] L. D. Landau and E. M. Lifshitz, *Electrodynamics of Continuous Media*, Their Course on Theoretical Physics, Vol. 8 (Pergamon, Oxford, UK, 1960).

[4] G. Łach, M. DeKieviet, and U. D. Jentschura, Multipole Effects in atom-surface interactions: A theoretical study with an application to He–α-quartz, Phys. Rev. A **81**, 052507 (2010).

[5] V. Druzhinina and M. DeKieviet, Experimental Observation of Quantum Reflection Far from Threshold, Phys. Rev. Lett. **91**, 193202 (2003).

[6] G. Dufour, A. Gérardin, R. Guérout, A. Lambrecht, V. V. Nesvizhevsky, S. Reynaud, and A. Yu. Voronin, Quantum reflection of antihydrogen from the Casimir potential above matter slabs, Phys. Rev. A **87**, 012901 (2013).

[7] V. Sandoghdar, C. I. Sukenik, E. A. Hinds, and S. Haroche, Direct Measurement of the Van Der Waals Interaction between an Atom and its Images in a Micron-Sized Cavity, Phys. Rev. Lett. **68**, 3432 (1992).

[8] C. I. Sukenik, M. G. Boshier, D. Cho, V. Sandoghdar, and E. A. Hinds, Measurement of the Casimir-Polder Force, Phys. Rev. Lett. **70**, 560 (1993).

[9] G. Barton, Quantum-electrodynamic level shifts between parallel mirrors: Analysis, Proc. R. Soc. London, Ser. A **410**, 141 (1987).

[10] G. Barton, Quantum-electrodynamic level shifts between parallel mirrors: Applications, mainly to Rydberg states, Proc. R. Soc. London, Ser. A **410**, 175 (1987).

[11] H. Friedrich, G. Jacoby, and C. G. Meister, Quantum reflection by Casimir–van der Waals potential tails, Phys. Rev. A **65**, 032902 (2002).

[12] V. B. Bezerra, G. L. Klimchitskaya, V. M. Mostepanenko, and C. Romero, Lifshitz theory of atom-wall interaction with applications to quantum reflection, Phys. Rev. A **78**, 042901 (2008).

[13] M. Antezza, L. P. Pitaevskii, and S. Stringari, Effect of the Casimir-Polder force on the collective oscillations of a trapped Bose-Einstein condensate, Phys. Rev. A **70**, 053619 (2004).

[14] C. Moore, C. M. Adhikari, T. Das, L. Resch, C. A. Ullrich, and U. D. Jentschura, Temperature-dependent dielectric function of intrinsic silicon: Analytic models and atom-surface potentials, Phys. Rev. B **106**, 045202 (2022).

[15] H. A. Bethe, The electromagnetic shift of energy levels, Phys. Rev. **72**, 339 (1947).

[16] U. D. Jentschura and P. J. Mohr, Calculation of hydrogenic Bethe logarithms for Rydberg states, Phys. Rev. A **72**, 012110 (2005).

[17] U. D. Jentschura and G. S. Adkins, *Quantum Electrodynamics: Atoms, Lasers and Gravity* (World Scientific, Singapore, 2022).

[18] U. D. Jentschura, Long-range atom-wall interactions and mixing terms: Metastable hydrogen, Phys. Rev. A **91**, 010502(R) (2015).

[19] W. H. Press, B. P. Flannery, S. A. Teukolsky, and W. T. Vetterling, *Numerical Recipes in C: The Art of Scientific Computing*, 2nd ed. (Cambridge University Press, Cambridge, UK, 1993).

[20] W. Sellmeier, Ueber die durch die Aetherschwingungen erregten Mitschwingungen der Körpertheilchen und deren Rückwirkung auf die ersteren, besonders zur Erklärung der Dispersion und ihrer Anomalien, Ann. Phys. (Leipzig) **223**, 386 (1872).

[21] A. Deinega and S. John, Effective optical response of silicon to sunlight in the finite-difference time-domain method, Opt. Lett. **37**, 112 (2012).

[22] K. Prokopidis and C. Kalialakis, Physical interpretation of a modified Lorentz dielectric function for metals based on the Lorentz–Dirac force, Appl. Phys. B: Lasers Opt. **117**, 25 (2014).

[23] H. Choi, J.-W. Baek, and K.-Y. Jung, Comprehensive study on numerical aspects of modified Lorentz model-based dispersive FDTD formulations, IEEE Trans. Antennas Propag. **67**, 7643 (2019).

[24] K. Pachucki, Higher-order binding corrections to the Lamb shift, Ann. Phys. (NY) **226**, 1 (1993).

[25] U. Jentschura and K. Pachucki, Higher-order binding corrections to the Lamb shift of $2P$ states, Phys. Rev. A **54**, 1853 (1996).

[26] F. Reiche and W. Thomas, Über die Zahl der Dispersionselektronen, die einem stationären Zustand zugeordnet sind, Z. Phys. **34**, 510 (1925).

[27] W. Kuhn, Über die Gesamtstärke der von einem Zustande ausgehenden Absorptionslinien, Z. Phys. **33**, 408 (1925).

[28] U. D. Jentschura, S. Kotochigova, E.-O. Le Bigot, P. J. Mohr, and B. N. Taylor, Precise Calculation of Transition Frequencies of Hydrogen and Deuterium Based on a Least-Squares Analysis, Phys. Rev. Lett. **95**, 163003 (2005).

[29] E. Masina, Useful review on the Exponential-Integral special function, arXiv:1907.12373.